

Self-lubrication and tribological properties of SBA-15 as smart microcontainer and resin composites

Yiming Sun¹ | Yilong Ren² | Lina Zhu^{1,3}  | Lina Si⁴ | Jiajie Kang^{1,3}  | Guoxin Xie²

¹School of Engineering and Technology, China University of Geosciences, Beijing, China

²State Key Laboratory of Tribology, Tsinghua University, Beijing, China

³Zhengzhou Institute, China University of Geosciences Beijing, Zhengzhou, People's Republic of China

⁴School of Mechanical and Materials Engineering, North China University of Technology, Beijing, China

Correspondence

Lina Zhu, School of Engineering and Technology, China University of Geosciences, Beijing 100083, China.
Email: zhulina@cugb.edu.cn

Lina Si, School of Mechanical and Materials Engineering, North China University of Technology, Beijing 100144, China.
Email: silina_thu@163.com

Funding information

Beijing Natural Science Foundation of China, Grant/Award Number: JQ21008 3212003; Natural Science Foundation of China, Grant/Award Number: 51775044; Tsinghua-Foshan Innovation Special Fund, Grant/Award Number: 2020THFS0127

Abstract

In this work, we showed that the mesoporous molecular sieve SBA-15 could be used as an oil storage smart microcontainer to adsorb PAO6 oils and is prepared as an oil-containing molecular sieve SBA-15O, the compositing of SBA-15O with unsaturated polyester resins (UPR) can significantly improve the lubrication properties of UPR. The oil-containing molecular sieve SBA-15O was prepared by vacuum impregnation and compounded into the UPR. The lubricating effect of different SBA-15O contents on the UPR was investigated. As compared with the UPR, the coefficient of friction (COF) of the 10%SBA-15O/UPR could be reduced to 10% of that without SBA-15O, and the wear rate by three orders of magnitude. The results show that the improvement of lubricating performance is related to the release of lubricating oil from the microcontainer to the surface to produce a lubricating oil film during friction, thereby enhancing the self-lubricating performance of the composite material.

KEYWORDS

composites, friction, SBA-15, self-lubricating, unsaturated polyester resins

1 | INTRODUCTION

Unsaturated polyester resins (UPR) are a commonly used thermosetting resin,^[1,2] generally made of unsaturated diacid and diol or saturated diacid and unsaturated diol condensation of linear polymer compounds with ester bonds and unsaturated double bonds.^[3] It has good mechanical properties, chemical resistance, and electrical insulation properties and can be widely used in the automotive, electronics, and chemical industries.^[4–6]

Polymer-based self-lubricating materials have been of great interest to researchers because of their excellent

tribological properties and their ability to be filled with different fillers depending on the requirements.^[7,8] In recent years, smart materials with stimulus–response properties have attracted significant research interest in the fields of electronics, catalysis, and tribology.^[9–12] These materials can produce functional changes in response to an applied stimulus (e.g., changes in temperature, stress, electric field, pH, and other environmental changes) to achieve the desired effect.^[13–15] For example, while conventional material workpiece lubrication is usually achieved by adding lubricant directly to the contact interface, smart lubricating materials can achieve the

effect of interfacial lubrication by releasing the lubricant embedded in the composite material when subjected to external temperature and stress changes.^[16,17] For these smart composites, one of the most important factors is the development of depot systems compounded into the matrix that can release the lubricant as required. Zhang et al.^[18] synthesized and prepared mesoporous metal-organic frameworks (m-MOFs) as smart nanocontainers and adsorbed alkylamines as lubricants, which were compounded with epoxy resins to prepare self-lubricating nanocomposites with ultra-low coefficients of friction.

Zeolite molecular sieves are a class of porous inorganic aluminosilicate materials with a porous microstructure, excellent thermodynamic properties, and chemical stability, with adsorption of gases and liquids being one of their most prominent applications.^[19,20] In recent decades, they have received much attention as absorbent materials.^[21] The use of zeolite molecular sieves as intelligent storage systems for absorbent storage lubricants with porous microstructures compounded with polymeric materials can avoid irreversible damage to the storage systems to some extent. Ji et al.^[22] compositing ZSM-5 zeolite molecular sieves with PEEK to prepare porous PEEK composites with excellent mechanical properties, tribological properties, and anti-adhesion properties.

SBA-15 molecular sieve is a pure silicon molecular sieve with the advantages of large pore size, thick pore wall, and good hydrothermal stability. This work is devoted to using SBA-15 as a smart microcontainer, storing PAO6 as a lubricant in the pores of molecular sieves by vacuum impregnation, and then compositing with the matrix material (UPR) to prepare a composite material with good tribological properties. Based on macroscopic frictional experiments with the ball-on-disc configuration, the lubricating properties of the composites were systematically studied. The results show that this composite material has good lubricating properties.

2 | EXPERIMENTAL

2.1 | Materials

SBA-15 molecular sieve was purchased from Nanjing Xianfeng Nanomaterials Technology Co., Ltd., UPR (m-phenylene unsaturated polyester resin, model: 199), catalyst cobalt naphthenate, and curing agent MEKP were purchased from Jiangyin Wanqian Chemical Co., Ltd. Company, toluene was provided by Beijing Tongguang Fine Chemical Company, ethanol was supplied by Beijing Chemical Plant, and PAO6 was purchased from Shandong Yousuo Chemical Technology Company.

2.2 | Preparation of SBA-15/UPR composites

The composite material is prepared as shown in Figure 1. At room temperature, a certain amount of SBA-15 molecular sieve is impregnated in PAO6 synthetic base oil by vacuum impregnation, stirred well, and then put into a vacuum chamber for impregnation. Because PAO6 is easily soluble in toluene, the residual PAO6 on the surface of the molecular sieve is cleaned with toluene after the impregnation is completed, and then the surface is rinsed with ethanol, and then put into the oven for drying at 80°C for 2 h, SBA-15 porous oil-containing molecular sieve was prepared. Mix SBA-15 with 199 unsaturated polyester resin in a specific ratio. The content of the SBA-15 molecular sieve was 0, 4, 6, 8, 10, and 15 wt%, respectively, and magnetic stirring for 30 min was used to form a good suspension. Then add 1% accelerator cobalt naphthenate and 2% curing agent MEKP, continue to stir for 5 min. After the stirring is completed, pour the suspension into the rubber mold, degas under vacuum, and the sample is cured at 80°C for 4 h.

2.3 | Materials characterization

Transmission electron microscopy (TEM, JEM-2100Plus) was used to observe the molecular sieve's particle size and pore size. The average pore size and specific surface area of SBA-15 molecular sieves were tested by surface area and pore size analyzer (BET, SIMP). The compression properties of the composites were tested with the electronic universal testing machine (WDW3020-20KN, Kason Group). The material wear areas were characterized by environmental scanning electron microscopy (ESEM, FEI Quanta 200 FEG). The three-dimensional appearances of wear scar and the wear rate were obtained by using the three-dimensional white light interference surface topography device (Zygo Nexvie).

The UMT-3 universal micro-friction and wear tester from CETR Corporation was used to test the friction properties of the composites. The counterpart balls were Gcr15 steel balls, 4 mm in diameter, which were thoroughly cleaned with ethanol before each test. The reciprocating friction stroke was 5 mm, the sliding speed was 20 and 50 mm/s, and the test loads were 3 and 10 N. The wear volume, ΔV , was measured by a three-dimensional white light interference surface topography device (Zygo NexView) after friction tests, and hence the specific wear rate, the calculation formula is shown in Equation (1)

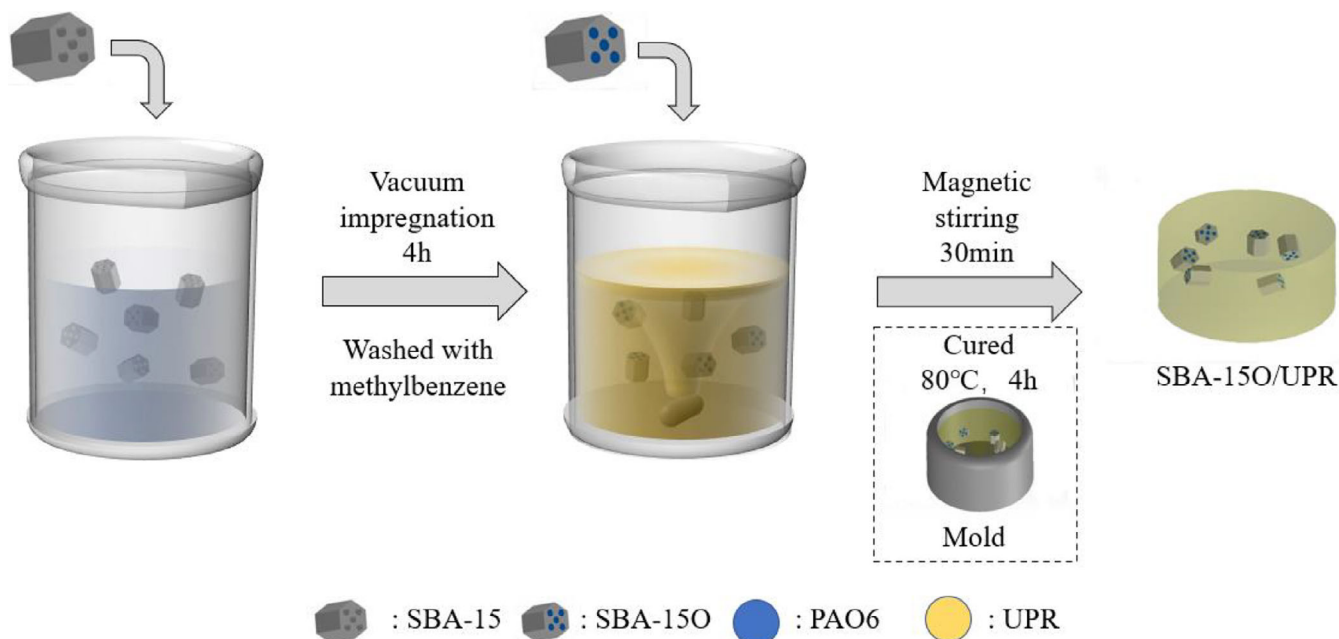


FIGURE 1 Synthesis process for the SBA-150/UPR

$$W_s = \frac{\Delta V}{F_N d} \quad (1)$$

where F_N is the normal load applied on the Gcr15 steel ball during sliding, and d is the total sliding distance.

3 | RESULTS AND DISCUSSION

3.1 | Characterization of SBA-15

The SBA-15 was ultrasonically dispersed, and the molecular sieve was observed by transmission electron microscope. The TEM results are shown in Figure 2. We can see that the particle size of the SBA-15 is about 1 μm , and the internal pore distribution is uniform and regular. The average pore size of most of these molecular sieves was found to be close to 11 nm (Figure 2A,C), with a small number of particles having a pore size of 6 nm (Figure 2E).

The nitrogen adsorption-desorption curves and pore size distribution of the SBA-15 without adsorbed oil are shown in Figure 3. As shown in Figure 3A, molecular sieves exhibit typical type IV isotherms, and type IV curves are typical of mesoporous materials.^[23] The isotherm contains an H1-type hysteresis loop, with a gentle increase in adsorption in the low-pressure section, when nitrogen molecules are adsorbed on the inner surface of the mesopores in a monolayer to multilayer. There is a sudden increase in adsorption around $p/p_0 = 0.7-0.9$, and this section reflects the

sample pore size. The pore size distribution of the molecular sieve can be obtained from the calculation, as shown in Figure 3B. The calculated average pore size is 9.597 nm, which is consistent with the TEM results, with a specific surface area of 687.679 m^2g^{-1} and a pore volume of 1.341 cm^3g^{-1} .

3.2 | SBA-150 molecular sieve oil content analysis

The results of the thermogravimetric testing of the oil content of the SBA-150 are shown in Figure 4. In order to explore the suitable impregnation time, firstly, SBA-15 was impregnated in PAO6 for different times, and after impregnation, the surface oil stain was cleaned uniformly with toluene, and the amount of toluene and oil was 1:1. The test results are shown in Figure 4A,B, and the oil content of the three groups of 2, 4, and 6 h on the surface was similar, all being about 30.5%, and increasing the impregnation time had little effect on the oil content. Therefore, a 4 h impregnation time was chosen to test the change of oil content after reducing the amount of toluene. The toluene to oil ratios of 1:1, 1:2, and 1:4 were chosen for the experiments. When the toluene dosage continued to decrease, the molecular sieve would not be cleaned, so a vacuum impregnation of 4 h and toluene to oil ratio of 1:4 was finally chosen as the desired experimental parameters to continue the subsequent experiments.

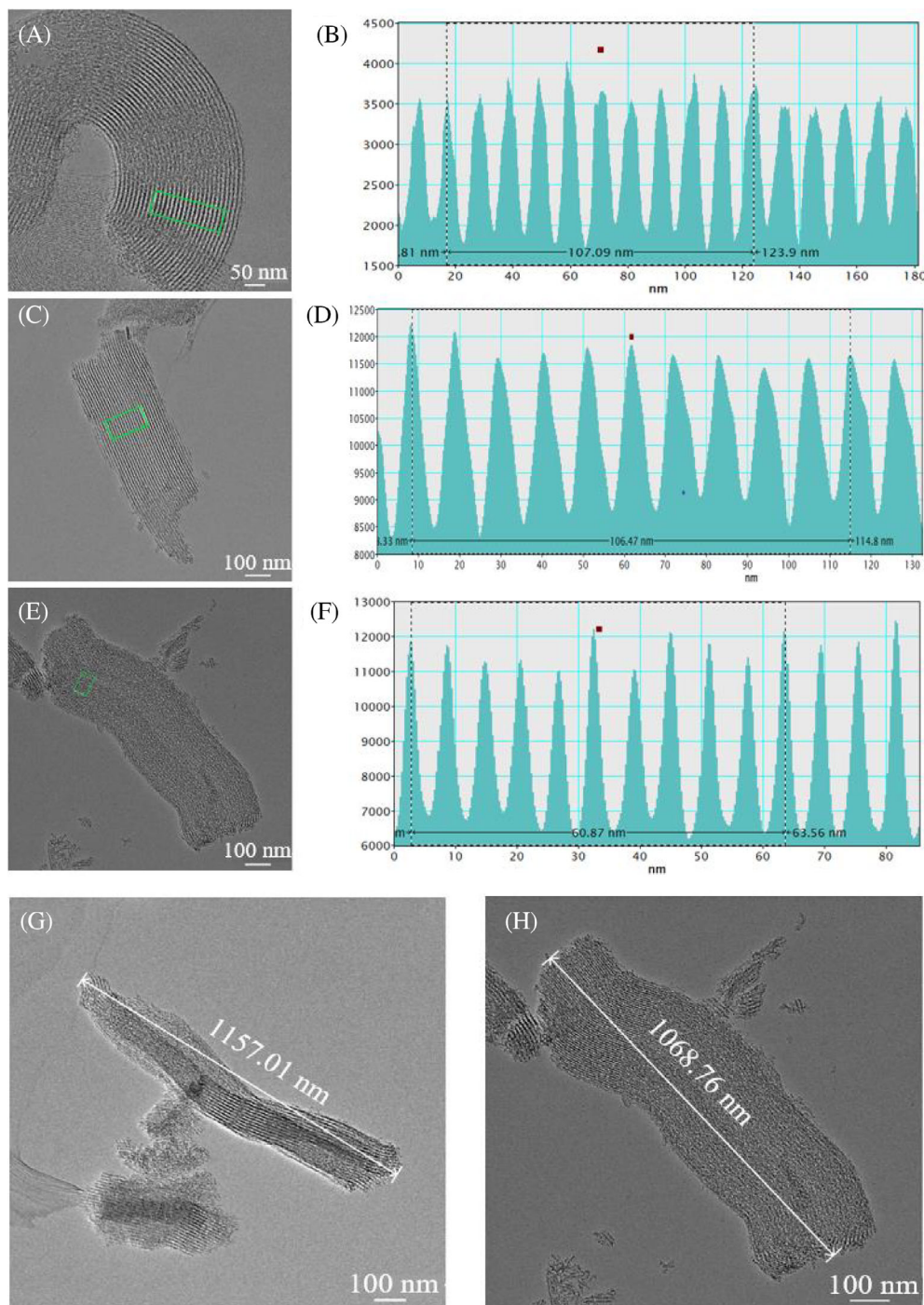


FIGURE 2 (A, C, E, G, H) TEM images of SBA-15 molecular sieve (B, D, F) pore spacing images for the green area section of (A, C, E)

3.3 | Mechanical properties test of SBA-15O/UPR composites

To investigate the effect of SBA-15O molecular sieves on the mechanical properties of the composites, this section investigates the effects of different mass fraction contents of SBA-15O/UPR composites (pure UP, 4 wt% SBA-15O/UP, 6 wt% SBA-15O/UPR, 8 wt% SBA-15O/UPR, 10 wt% SBA-15O/UPR, 15wt.%SBA-15O/UPR) were tested for their compression strength. Figure 5A shows

typical stress–strain curves for composites with different molecular sieve contents. It can be seen from the figure that the stress–strain curves of pure UPR and composites filled with 4, 6, 8, 10, and 15 wt% oil-containing molecular sieves follow a similar trend. At the same time, the stress tends to increase and then decrease with increasing molecular sieve filling. The relationship between the compressive strength of the composites and the amount of molecular sieve added is shown in Figure 5B, which shows that the compressive strength of the composites

FIGURE 3 (A) N_2 adsorption–desorption isotherms of SBA-15 (B) pore size distribution of SBA-15

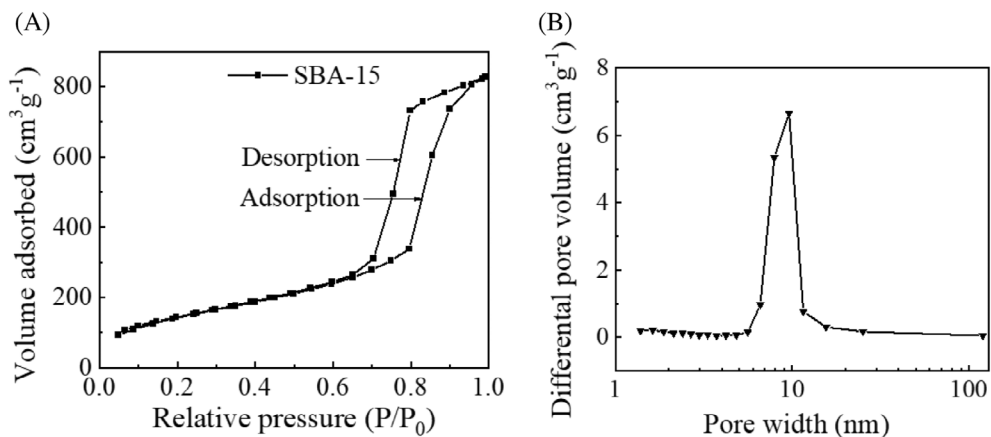


FIGURE 4 Oil content thermogravimetric test of SBA-15O (A, B) SBA-15 vacuum impregnation for different times (C, D) different ratio of toluene to oil for cleaning of SBA-15

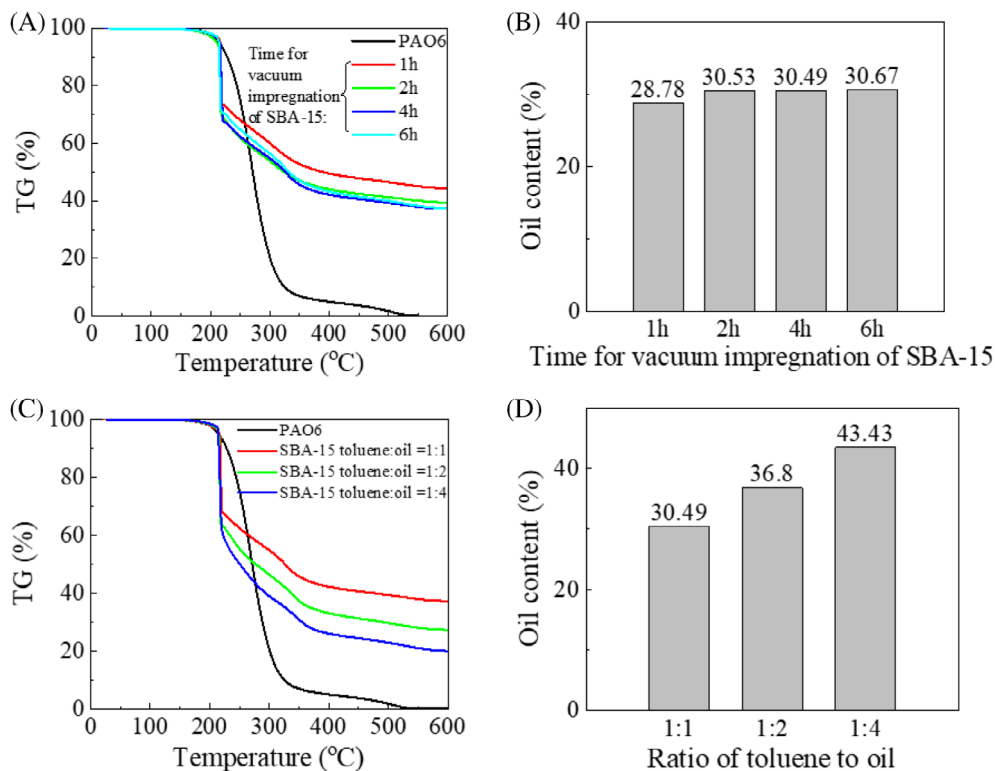
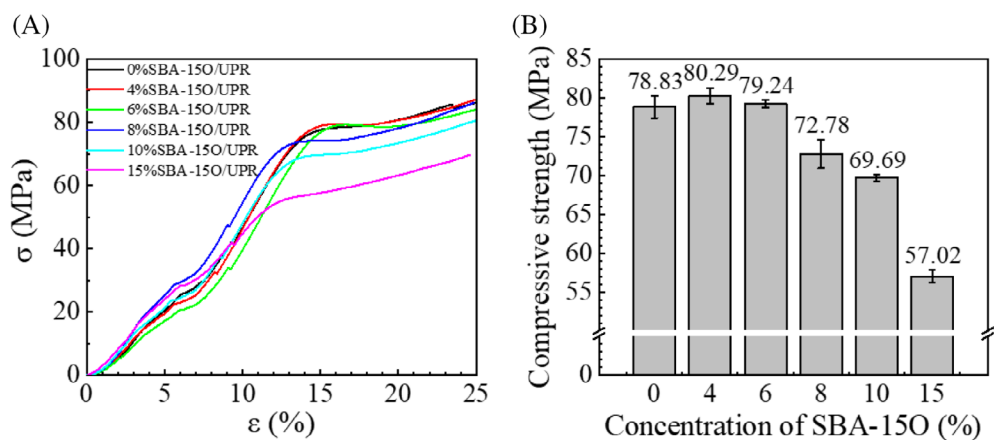


FIGURE 5 (A) Typical stress–strain curves for the composites with different SBA-15O contents (B) compressive strengths of SBA-15O/UPR composites



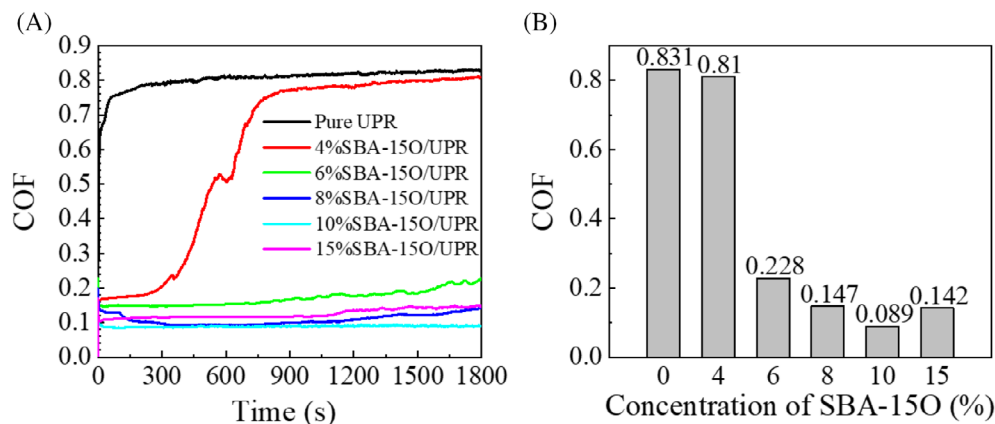


FIGURE 6 (A) Typical COF curves for composites with different SBA-150 contents (B) tribological properties of SBA-150/UPR composites

tends to increase slightly and then decrease as the amount of oil-containing molecular sieve is added. The compressive strength of the composites is the lowest when the amount of molecular sieve added is 15 wt%, only 57.02 MPa. This is mainly due to two reasons: on the one hand, the molecular sieve is mainly composed of hard particles, a small amount of molecular sieve can enhance the strength of the material; but an excessive amount of molecular sieve makes the interfacial adhesion between the particles and the matrix poor^[24] which makes the compression strength of the material decrease significantly. on the other hand, the increase of molecular sieve content causes the increase of the porosity of the composite^[25] which also makes the compression strength of the material decrease.

3.4 | Tribological properties of composite materials

The results are shown in Figure 6. The tribological performance of pure UPR was poor, with a friction coefficient as high as 0.831. At a molecular sieve content of only 4% with oil, the coefficient of friction of the composite showed an increasing trend, and the final friction coefficient reached 0.81, which was similar to that of pure UP. The friction coefficient of the composite decreases significantly as the content of the SBA-150 molecular sieve with oil continues to increase, reaching an optimum coefficient of friction of 0.089 at 10% and a slight increase when the molecular sieve content continues to increase to 15%.

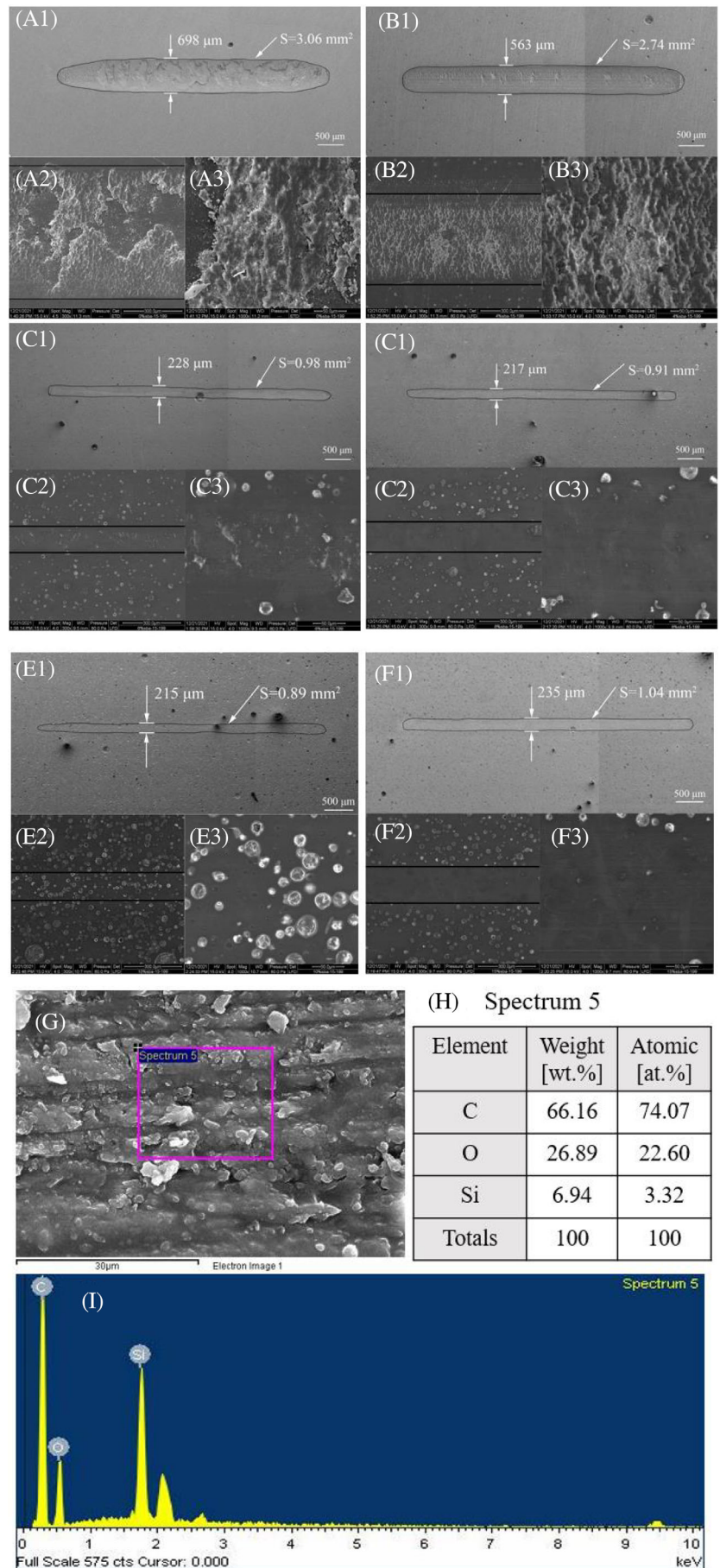
3.5 | Characterization and analysis of wear mark area

The morphology of the wear on the composite surface helps to analyze the tribological properties of the material better; therefore, the wear surface morphologies of the

pure UP and SBA-150/UPR composites are shown in Figure 7. The black areas are the wear areas of the material. In Figure 7A, layer separation and more cracks appear on the surface of the unfilled UP and the 4% SBA-150/UPR composite. The two groups of materials have a high coefficient of friction, a scarcity of oil lubrication, and adhesive delamination on the surface of the composites under external loads during frictional reciprocating motion^[26] On the UPR surface with 6 wt% SBA-150, only some shallow grooves and small cracks could be seen on the wear surface, as shown in Figure 7C, indicating the presence of slight abrasive wear. In contrast, only minor abrasion was seen on the UPR surfaces with 8 wt% SBA-150 and 15% wt% SBA-150 (Figure 7D,F). On the surface of the UPR with 10 wt% SBA-150, the abrasion marks were slight and almost invisible. These results indicate that the effect of increasing oil content with increasing oil-containing molecular sieve content and the continuous seepage of lubricant from the pores during friction to form a frictional contact zone is optimal at 10 wt% molecular sieve content. However, the composites containing 15 wt% SBA-150 oil-containing particles exhibit an increased COF, mainly due to the softening of the surface of the UPR matrix as the mechanical properties of the material decrease due to the higher amount of lubricant in the UPR matrix. Under the action of external loads during friction, the UPR composite matrix undergoes elastic deformation. The actual contact area between the steel ball and the composite increases, increasing frictional resistance increasing COF. As shown in Figure 7G, the EDS of 10% SBA-150/UPR composites cross section was performed. SBA-15 molecular sieve is a pure silicon molecular sieve, Si is the main element in SBA-15. The results indicate that SBA-150 is present inside the UPR rather than on the surface.

As the above friction and wear experiments, the experimental load is 3 N, the sliding speed is 20 mm/s, the resulting wear marks are shallow, under the three-dimensional white light interferometry surface

FIGURE 7 SEM image of wear area of composite material. {Magnification: 1: [$\times 30$], 2: [$\times 300$], 3: [$\times 1000$]} (A) pure UPR (B) 4% SBA-150/UPR (C) 6% SBA-150/UPR (D) 8% SBA-150/UPR (E) 10% SBA-150/UPR (F) 15% SBA-150/UPR; (G), (H) and (I) the EDS of 10% SBA-150/UPR composites cross section



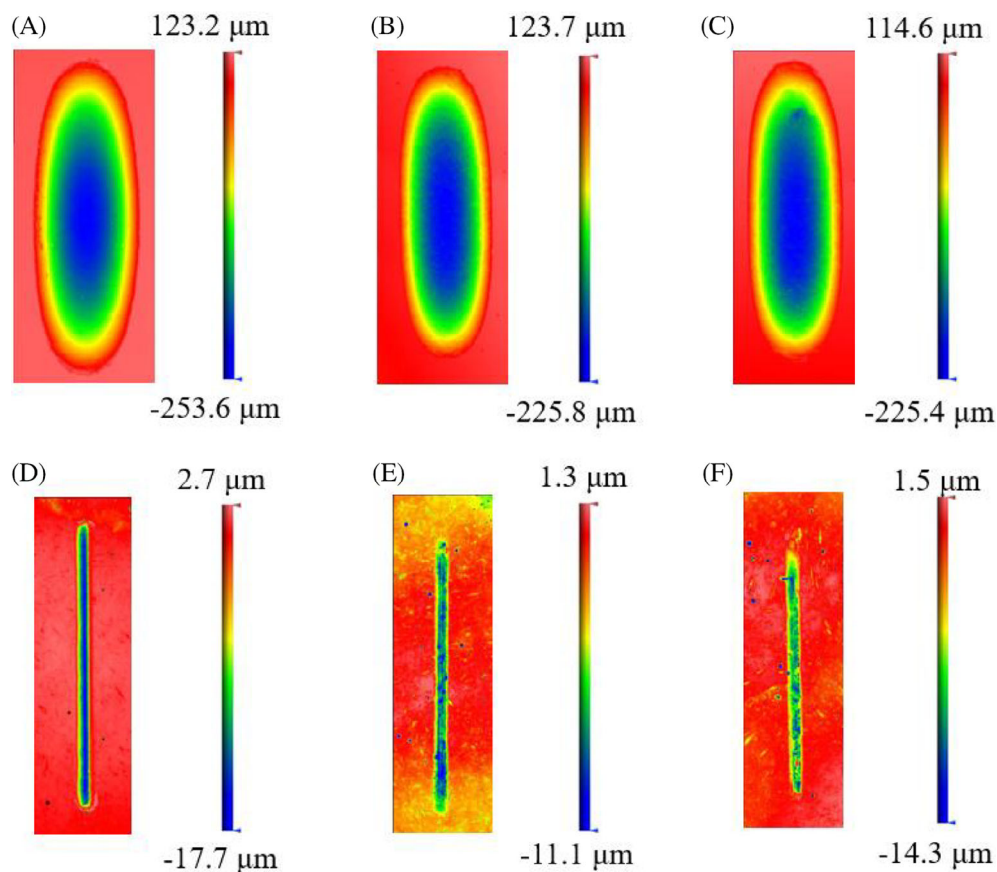


FIGURE 8 2D white light interference morphologies of composite wear marks (A) pure UPR (B) 4% SBA-150/UPR (C) 6% SBA-150/UPR (D) 8% SBA-150/UPR (E) 10% SBA-150/UPR (F) 15% SBA-150/UPR

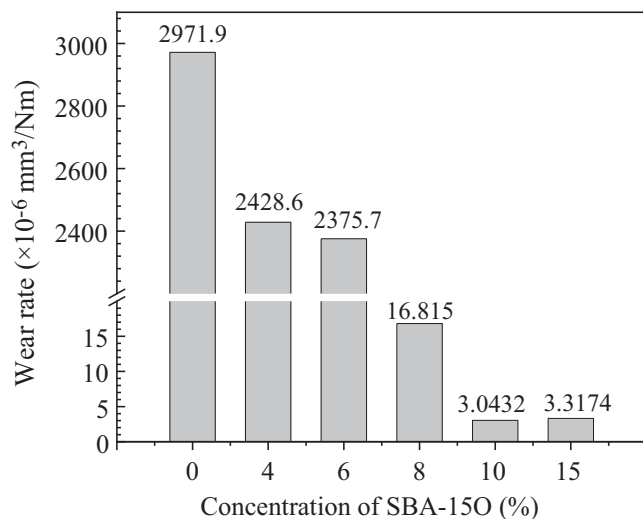


FIGURE 9 Wear rates of composites with different SBA-150 contents

morphology observation wear marks are not obvious, cannot calculate its wear rate, so increase the experimental load and sliding speed, the experimental load to 10 N, sliding speed to 50 mm/s, in this more severe working conditions to calculate its wear rate. The results are shown in Figure 8.

Under higher loads and faster sliding speeds, the material wear marks were characterized. Because of the more severe conditions. Adhesion delamination occurs during friction, and the friction coefficient increases, which is similar to the depth of the wear scar of the first two groups of materials. 6% of the SBA-150/UPR composite material did not contain enough oil to provide good lubrication. The 8% SBA-150/UPR, 10% SBA-150/UPR, and 15% SBA-150/UPR groups, on the other hand, had good lubrication properties, and the wear rate decreased by three orders of magnitude compared to the previous groups (Figure 9).

3.6 | Mechanism analysis

The self-lubricating mechanism of composites is mainly to form a boundary lubricating film on the wear surface. As shown in Figure 10, the SBA-150 smart micro-container with automatic feedback function was introduced into the UPR matrix. The micro-container molecular sieve used for storing lubricating oil can quickly respond to changes caused by external pressure. When the composite material is in working state The PAO6 stored in the pores of SBA-150 is precipitated in a

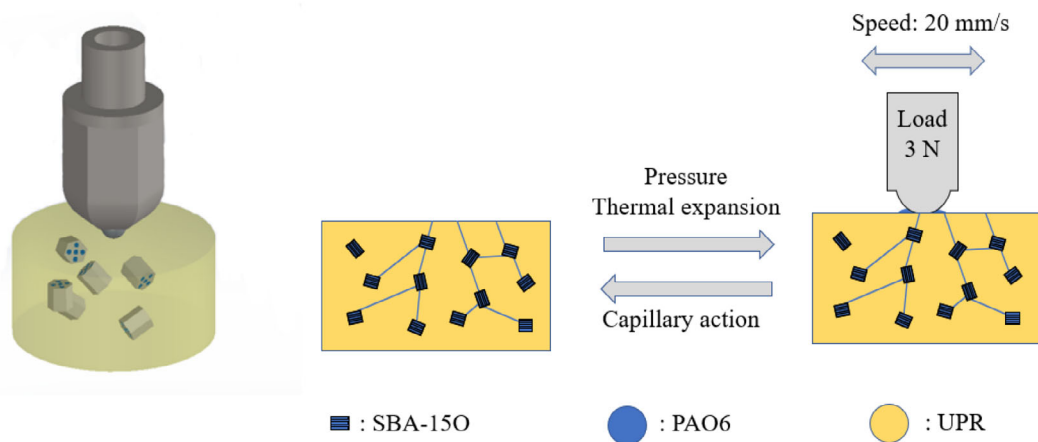


FIGURE 10 Lubrication mechanism diagram of lubricating oil release

small amount due to the combined effect of pressure and thermal expansion^[27] which lubricates the frictional contact area and plays the role of lubrication and friction reduction. And because of the capillary action of the pores of the composite material,^[28] after the friction is over, the small amount of lubricant on the surface will flow back into the pore structure after the friction is over, achieving the effect of intelligent lubrication.^[29] The PAO6 released from the SBA-150 microcontainer effectively lubricates the friction surfaces. The resulting boundary lubricating oil film plays the role of lubricating the surface of the friction pair and reduces the COF of the material.

4 | CONCLUSION

The oil-containing molecular sieve SBA-150 was prepared by vacuum impregnation and compounded into the UPR matrix. The lubricant effect of different SBA-150 contents on the UPR was investigated. Among them, the 10% SBA-150/UPR composite was the best, with a coefficient of friction of 0.089 and a wear rate of $3.0432 \times 10^{-6} \text{ mm}^3/\text{Nm}$. The wear rate has been reduced by three orders of magnitude compared to pure UPR. There is a slight reduction in the mechanical strength, with the compressive strength decreasing from 78.83 to 69.69 MPa. The results show that the improvement in lubrication performance is related to the release of lubricating oil from the microcontainer to the surface of the friction subsets during friction to produce a lubricating oil film and that the composites have good self-lubricating properties.

ACKNOWLEDGMENTS

This work was supported by the Beijing Natural Science Foundation of China (grant nos. JQ21008 and 3212003), Natural Science Foundation of China (grant no. 51775044) and the Tsinghua-Foshan Innovation Special Fund (TFISF) (grant no. 2020THFS0127).

ORCID

Lina Zhu  <https://orcid.org/0000-0003-1742-1904>

Jiajie Kang  <https://orcid.org/0000-0002-8873-3684>

REFERENCES

- [1] S. Mishra, A. K. Mohanty, L. T. Drzal, M. Misra, S. Parija, S. K. Nayak, S. S. Tripathy, *Compos. Sci. Technol.* **2003**, 63(10), 1377.
- [2] C. Hengzhi, T. Xiaoxue, L. Jing, *Polymers* **2018**, 10, 362.
- [3] J. Molina, A. Laroche, J. V. Richard, A. S. Schuller, C. Rolando, *Front Chem* **2019**, 7, 375.
- [4] C. Liu, C. Wang, J. Tang, J. Zhang, Q. Shang, Y. Hu, H. Wang, Q. Wu, Y. Zhou, W. Lei, Z. Liu, *Polymer* **2018**, 10, 1288.
- [5] G. Peng, Q. Li, Y. Yang, H. Wang, W. Li, *Polym. Adv. Technol.* **2010**, 19, 1629.
- [6] Y. Bautista, A. Gozalbo, S. Mestre, V. Sanz, *Materials* **2018**, 11(1), 22.
- [7] P. Li, Z. Zhang, Z. Zhang, M. Yang, J. Yuan, W. Jiang, *Polym. Compos.* **2021**, 42, 5839.
- [8] S. C. Yan, Y. H. Xue, *Polym. Compos.* **2021**, 42, 4517.
- [9] M.-C. Daniel, D. Astruc, *Chem. Rev.* **2004**, 104, 293.
- [10] H. Fan, A. Wright, J. Gabaldon, A. Rodriguez, C. J. Brinker, Y. B. Jiang, *Adv. Funct. Mater.* **2006**, 16(7), 891.
- [11] E. S. Gil, S. M. Hudson, *Prog. Polym. Sci.* **2004**, 29(12), 1173.
- [12] S. Gao, J. Sun, P. Liu, F. Zhang, W. Zhang, S. Yuan, J. Li, J. Jin, *Adv. Mater.* **2016**, 28(26), 5307.
- [13] L. K. Ista, S. Mendez, V. H. Pérez-Luna, G. P. López, *Langmuir* **2001**, 17(9), 2552.

- [14] A. Fischer, A. Brembilla, P. Lochon, *Macromolecules* **2015**, 32(19), 6069.
- [15] D. Li, H. Qiang, J. Li, *Adv. Colloid Interf. Sci.* **2009**, 149(1–2), 28.
- [16] M. Kano, *Tribol. Int.* **2006**, 39(12), 1682.
- [17] Y. A. Han, Z. A. Lin, L. A. Hao, X. Fan, M. Zhu, *Carbon* **2020**, 157, 217.
- [18] G. Zhang, G. Xie, L. Si, S. Wen, D. Guo, *ACS Appl. Mater. Interfaces* **2017**, 9, 38146.
- [19] M. E. Davis, *Nature* **2010**, 33(40), 245.
- [20] M. S. Shah, M. Tsapatsis, J. I. Siepmann, *Chem. Rev.* **2017**, 117, 7b00095.
- [21] G. Kalies, R. Rockmann, D. Tuma, J. Gapke, *Appl. Surf. Sci.* **2010**, 256(17), 5395.
- [22] Z. Ji, G. Xie, W. Xu, S. Wu, L. Zhang, J. Luo, *Adv Mater Interfaces* **2019**, 6(10), 1801889.
- [23] X. Zhang, Y. Guo, H. Chen, W. Zhu, P. Zhang, *J. Mater. Chem. A* **2014**, 2(24), 9002.
- [24] A. C. Manalo, E. Wani, N. A. Zukarnain, W. Karunasena, K.-T. Lau, *Compos. Part B* **2015**, 80, 73.
- [25] Q. Li, Y. Zhang, D. Wang, H. Wang, G. He, *Mater. Des.* **2017**, 116, 171.
- [26] C. Dong, L. Shi, L. Li, X. Bai, C. Yuan, Y. Tian, *Tribol. Int.* **2017**, 106, 55.
- [27] M. Marchetti, M. H. Meurisse, P. Vergne, J. Sicre, M. Durand, *Tribol. Lett.* **2001**, 10(3), 163.
- [28] M. Shao, S. Li, C. Duan, Z. Yang, C. Qu, Y. Zhang, D. Zhang, C. Wang, T. Wang, Q. Wang, *ACS Appl. Mater. Interfaces* **2018**, 10, 41699.
- [29] T. W. Di Zhang, C. W. Qihua Wang, *Appl. Polym* **2017**, 134, 45106.

How to cite this article: Y. Sun, Y. Ren, L. Zhu, L. Si, J. Kang, G. Xie, *Polym. Compos.* **2022**, 1.
<https://doi.org/10.1002/pc.26932>